

Optimization of Single-layer Absorber on Constrained Sound Absorption System by Using GA Algorithm

Ying-Chun Chang, Long-Jyi Yeh, Min-Chie Chiu, and Gaung-Jer Lai

Department of Mechanical Engineering, Tatung University

ABSTRACT

Noise is a main contributor to the psychological and physiological illnesses of workers; therefore, it is essential to have noise controlled in an enclosed space with high echo effects. Since the thickness of the sound absorber is usually restrictive, it becomes necessary to minimize the noise under space constraint. In this paper, the optimization of the single-layer absorber, together with genetic algorithm (GA), is presented. Before the optimization, a sample was tested and compared with the experimental data to check the accuracy of the mathematical models. It turned out that both results are in good agreement. This study provides a novel scheme with GA in the optimization of sound absorbers in a constrained sound absorption system.

Keywords: single-layer absorber, transfer matrix method, constrained sound absorption system, GA optimization

限制空間下的雙腔邊進排氣式消音器的外型最佳化設計

張英俊 葉隆吉 邱銘杰 賴光哲

大同大學機械工程學系

摘 要

噪音對工廠作業人員的生理及心理上的疾病有高度的影響，因此，對於具有高迴音的密閉系統而言，噪音控制益形顯得重要，然而，為保有維修空間，廠房內的吸音板厚度受到局限，如此一來，如何在有限空間下將音量控制至最小，便成為一有趣且值得探討的問題，本文將採用單層吸音板並結合遺傳演算法進行分析，在進行最佳化前，為驗證數學模式的正確性，將先進行一組樣本的吸音率實測並與理論值做比較，結果顯示，理論值與實測結果頗為吻合，本研究在解決局限空間系統下的吸音板最佳化設計上，確實提供一種嶄新的解決方法。

關鍵字:單層吸音板，傳輸矩陣法，侷限吸音系統，遺傳演算最佳化。

I. INTRODUCTION

During the past three decades, there has been a growing interest in problem solving algorithms inspired by natural systems in physics and biology. One of the best known algorithms is the genetic algorithms [1] which have been applied successfully into many disciplines. Genetic algorithm optimizers are robust, stochastic algorithms, whose search model mimics the genetic drift and Darwinian strife for survival. A great advantage of GA optimizers is that GA is able to locate the global optimum in a near optimal manner without either the first derivative of objective function or the starting point used in traditional deterministic methods. In practical optimization problems, such nearly optimal solution are usually acceptable because engineers prefer finding a satisfactory near optimal solution quickly rather than taking a long time to find a perfect solution which is only slightly or partially better [2].

In optimization, the evolution-based algorithms have been presented as innovative alternatives to traditional optimization techniques. In addition; the optimization of sound absorption system under space constraints is rarely accomplished, the interest in sound absorber's shape optimization to minimize the sound pressure level (SPL) inside the room by GA method is thus arising in the field.

In this paper, the theoretical sound absorption of sound absorber is deduced. Besides, the semi-empirical formula of specific normal impedance by Delany and Bazley [3] as well as by Bolt and Ingard [4, 5] are both included into the model derivation simultaneously. In addition, GA is encoded by MATLAB [6]. A numerical case of single layer sound absorber covered with perforated plate is also fully illustrated in the paper.

II. THEORETICAL BACKGROUND

For three-dimensional acoustic wave

propagating through a quiescent medium which is homogeneous and isotropic (with the rectangular partitions as shown in Fig.1 with b in length and h in width), three kinds of governing equations are

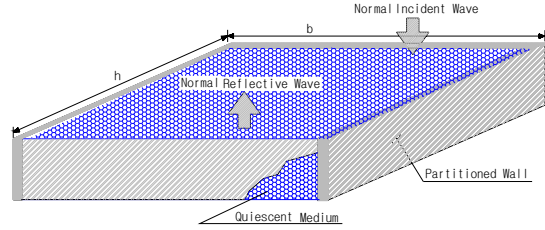


Fig. 1. Three dimensional wave propagating through a partitioned porous material.

I. Mass continuity equation:

$$\rho_o \nabla \cdot \vec{u} + \frac{D\rho}{Dt} = 0 \quad (1)$$

II. Momentum equation:

$$\rho_o \frac{D\vec{u}}{Dt} + \nabla p = 0 \quad (2)$$

III. Energy equation (isentropic):

$$\left(\frac{\partial p}{\partial \rho} \right)_s = \frac{\gamma(p_o + p)}{\rho_o + \rho} \approx \frac{\gamma p_o}{\rho_o} = c_o^2$$

or

$$\frac{p}{\rho} = c_o^2 \quad (3)$$

By partial derivation and substitution in Eqs. (1), (2) and (3), the wave governing equation yields

$$\left(\frac{D^2}{Dt^2} - c_o^2 \nabla^2 \right) p = 0 \quad (4)$$

where $\frac{D}{Dt} = \frac{\partial}{\partial t} + \vec{V}_o \cdot \vec{\nabla}$ is the total

derivative. \bar{V}_o is the mean velocity.

For Cartesian coordinate system (for rectangular ducts),

$$\nabla^2 = \frac{\partial^2}{\partial x^2} + \frac{\partial^2}{\partial y^2} + \frac{\partial^2}{\partial z^2} \quad (5)$$

By using separation of variables method, it yields

$$p(x, y, z, t) = \sum_{m=0}^{\infty} \sum_{n=0}^{\infty} \cos \frac{m\pi x}{b} \cos \frac{n\pi y}{h} \left(C_{1,m,n} e^{-jk_{z,m,n}^+ z} + C_{2,m,n} e^{+jk_{z,m,n}^- z} \right) e^{j\omega t} \quad (6)$$

$$u_z(x, y, z, t) = \frac{1}{\rho_o c_o} x \sum_{m=0}^{\infty} \sum_{n=0}^{\infty} \cos \frac{m\pi x}{b} \sin \frac{n\pi y}{h} \left(\frac{k_{z,m,n}^+}{k_o - Mk_{z,m,n}^+} C_{1,m,n} e^{-jk_{z,m,n}^+ z} + \frac{k_{z,m,n}^-}{k_o + Mk_{z,m,n}^-} C_{2,m,n} e^{+jk_{z,m,n}^- z} \right) e^{j\omega t} \quad (7)$$

with the compatibility condition

$$k_{x,m}^2 + k_{y,n}^2 + k_{z,m,n}^2 = (k_o + Mk_{z,m,n})^2 \quad (8a)$$

on

$$k_{z,m,n}^2 = (k_o + Mk_{z,m,n})^2 - \left(\frac{m\pi}{b} \right)^2 - \left(\frac{n\pi}{h} \right)^2 \quad (8b)$$

$$k_{z,m,n}^{\pm} = \frac{\mp Mk_o + \left[k_o^2 - (1-M^2) \left[\left(\frac{m\pi}{b} \right)^2 + \left(\frac{n\pi}{h} \right)^2 \right] \right]^{1/2}}{1-M^2} \quad (8c)$$

Consequently, only the plane wave at fundamental mode of (m=0, n=0) would propagate if the frequency is small enough so that

$$f < \frac{c_o}{2h} (1-M^2)^{1/2} \quad (9)$$

Where h is the larger value of the transverse dimensions of rectangular duct.

For one dimensional plane wave propagating perpendicularly through to a partitioned and uniform section with moving medium, the acoustic pressure is reduced to

$$p(z, t) = \left(C_1 e^{-jk_o z / (1+M)} + C_2 e^{+jk_o z / (1-M)} \right) e^{j\omega t} \quad (10)$$

The corresponding acoustic particle velocity is

$$u(z, t) = \left(\frac{C_1}{\rho_o c_o} e^{-jk_o z / (1+M)} - \frac{C_2}{\rho_o c_o} e^{+jk_o z / (1-M)} \right) e^{j\omega t} \quad (11)$$

Considering the boundary conditions of point 1 (z=0) and point 2 (z=L), it yields

$$\begin{pmatrix} p_1 \\ \rho_o c_o u_1 \end{pmatrix} = \begin{bmatrix} 1 & 1 \\ 1 & -1 \end{bmatrix} \begin{pmatrix} C_1 \\ C_2 \end{pmatrix} \quad (12)$$

$$\begin{pmatrix} p_2 \\ \rho_o c_o u_2 \end{pmatrix} = \begin{bmatrix} e^{-jk^+ L} & e^{jk^- L} \\ e^{-jk^+ L} & -e^{+jk^- L} \end{bmatrix} \begin{pmatrix} C_1 \\ C_2 \end{pmatrix} \quad (13)$$

where $k^+ = \frac{k_o}{1+M}$; $k^- = \frac{k_o}{1-M}$.

Combination of Eqs. (12) and (13) carries that

$$\begin{pmatrix} p_1 \\ u_1 \end{pmatrix} = e^{-j\frac{MkL}{1-M^2}x} \begin{bmatrix} \cos\left(\frac{kL}{1-M^2}\right) & jZ_2 \sin\left(\frac{kL}{1-M^2}\right) \\ j\frac{1}{Z_1} \sin\left(\frac{kL}{1-M^2}\right) & \cos\left(\frac{kL}{1-M^2}\right) \end{bmatrix} \begin{pmatrix} p_2 \\ u_2 \end{pmatrix} \quad (14)$$

For a plane wave with stationary medium of air, Eq. (14) is reduced to

$$\begin{pmatrix} p_1 \\ u_1 \end{pmatrix} = \begin{bmatrix} \cos(kL) & jZ_{air} \sin(kL) \\ j\frac{1}{Z_{air}} \sin(kL) & \cos(kL) \end{bmatrix} \begin{pmatrix} p_2 \\ u_2 \end{pmatrix} \quad (15)$$

Therefore, for a wave propagating normally into a stationary medium of “m”, the general matrix form between point 1 and point 2 is then expressed as

$$\begin{pmatrix} p_1 \\ u_1 \end{pmatrix} = \begin{bmatrix} \cos(k_m L) & jZ_m \sin(k_m L) \\ j\frac{1}{Z_m} \sin(k_m L) & \cos(k_m L) \end{bmatrix} \begin{pmatrix} p_2 \\ u_2 \end{pmatrix} \quad (16)$$

The absorber’s acoustic impedance on the perforated front plate is obtained from the bottom wall of the infinity of impedance [7]. The sound absorption mechanism of single layer perforated absorber is illustrated in Fig.2.

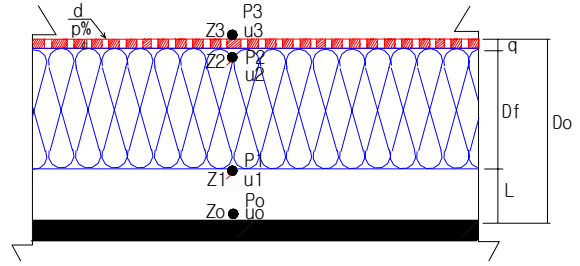


Fig.2 Sound absorbing mechanism for single layer perforated absorber.

As derived in Eq.(16), the relation of acoustic pressure p and acoustic mass velocity v between point 0 and point 1 is expressed as the transfer matrix shown below.

$$\begin{pmatrix} p_1 \\ u_1 \end{pmatrix} = \begin{bmatrix} \cos(\omega L / c_o) & i\rho_o c \sin(\omega L / c_o) \\ i\frac{\sin(\omega L / c_o)}{\rho_o c_o} & \cos(\omega L / c_o) \end{bmatrix} \begin{pmatrix} p_o \\ u_o \end{pmatrix} \quad (17)$$

Where p_1 is the acoustic pressure at the surface of the air layer, u_1 is the acoustic particle velocity at the surface of the air layer, p_o is the acoustic pressure at the absorber’s bottom, and u_o is the acoustic particle velocity at the back plate.

For a structure of “partitioned rigid wall + L thickness of air + Df thickness of the acoustic fiber”, the relation of acoustic pressure p and acoustic particle velocity u between point 1 and point 2 is expressed as the transfer matrix below.

$$\begin{pmatrix} p_2 \\ u_2 \end{pmatrix} = \begin{bmatrix} \cos[k_{fiber}(Df)] & jZ_{fiber} \sin[k_{fiber}(Df)] \\ j\frac{\sin[k_{fiber}(Df)]}{Z_{fiber}} & \cos[k_{fiber}(Df)] \end{bmatrix} \begin{pmatrix} p_1 \\ u_1 \end{pmatrix} \quad (18)$$

where $k_{fiber} = k_1 + jk_2$.

A complex form of Eq. (18) is expressed as

$$Z_2 = \frac{p_1 \cos[k_{fiber}(Df)] + ju_1 Z_{fiber} \sin[k_{fiber}(Df)]}{jp_1 \frac{\sin[k_{fiber}(Df)]}{Z_{fiber}} + u_1 \cos[k_{fiber}(Df)]} \quad (19)$$

By adopting the formula of specific normal impedance and wave number which is applied in fibrous material and derived by Delany and Bazley [3], Eq. (19) can thus be rearranged as

$$Z_2 = (R_{fiber} + jX_{fiber}) \frac{[\sinh(k_2) \cos(k_1) - j \sin(k_1) \cosh(k_2)]}{[\cos(k_1) \cosh(k_2) - j \sinh(k_2) \sin(k_1)]} \quad (20a)$$

where

$$\begin{aligned} k_1 &= \left[\frac{w(Df)}{c_o} \right] \left[1 + 0.0978 \left(\frac{\rho_o f}{R} \right)^{-0.700} \right] \\ ; \quad k_2 &= \left[\frac{w(Df)}{c_o} \right] \left[-0.189 \left(\frac{\rho_o f}{R} \right)^{-0.595} \right]; \\ R_{fiber} &= \left[\rho_o c_o \left(1 + 0.0571 \left(\frac{\rho_o f}{R} \right)^{-0.754} \right) \right]; \\ X_{fiber} &= \left[\rho_o c_o \left(-0.087 \left(\frac{\rho_o f}{R} \right)^{-0.732} \right) \right]. \end{aligned} \quad (20b)$$

Next, a structure of “partitioned rigid wall+ L thickness of air + Df thickness of acoustic fiber + q thickness of the perforated front plate” is analyzed. The normal impedance Z_3 at the surface of perforated front plate is expressed in the matrix form.

$$\begin{pmatrix} p_3 \\ u_3 \end{pmatrix} = \begin{bmatrix} \cos(k_p q) & jZ_p \sin(k_p q) \\ j \frac{\sin(k_p q)}{Z_p} & \cos(k_p q) \end{bmatrix} \begin{pmatrix} p_2 \\ u_2 \end{pmatrix} \quad (2)$$

1)

By developing Eq. (21) and adopting the formula of specific normal impedance and wave number of perforated plate derived by Bolt and Ingard [4,5], the normal impedance Z_3 at the surface of the perforated front plate is simplified into the complex form.

$$Z_3 = Z_p \frac{Z_2 + iZ_p \tan(k_p q)}{Z_p + iZ_2 \tan(k_p q)}$$

(22a)

where

$$\begin{aligned} Z_p &= j \frac{32\pi f M_h}{\left[1 + \frac{16M_h}{mN\pi^2 d^4} \right] [N\pi^2 d^4]}; \\ M_h &= \rho_o \left[\frac{\pi d^2 q}{4} + 2 \frac{d^3}{3} \right]. \end{aligned} \quad (22b)$$

For normal incidence, the sound absorption coefficient α [7,8] at f (1/1 Octave Band Centre frequency) is

$$\begin{aligned} \alpha_f &= 1 - \left| \frac{Z_3 - \rho_o c}{Z_3 + \rho_o c} \right|^2 \\ &= \alpha_f(Df, L, f, R, q, d, m, p\%) \end{aligned} \quad (23a)$$

(23a)

where $L = D_o - Df - q$. (23b)

For a rectangular room in which the sound absorbers are attached onto elected walls and ceiling of a rectangular room and the noisy equipment is located at $(X_{equip}, Y_{equip}, Z_{equip})$, the

sound pressure level SPL with respect the f -th octave centre frequency at receiver ($X_{receiver}, Y_{receiver}, Z_{receiver}$) is described as [8,9]

$$\begin{aligned}
 SPL_f &= SWL_f + 10 \log \left[\frac{Q}{4\pi r_1^2} + \frac{4}{RR_f} \right] \\
 &= SPL_f \left(\alpha_f, X_{room}, Y_{room}, Z_{room}, X_{receiver}, \right. \\
 &\quad \left. Y_{receiver}, Z_{receiver}, X_{equip}, Y_{equip}, Z_{equip} \right) \\
 &= SPL_f \left(f, p\%, Df, d, m, q, R, X_{room}, Y_{room}, Z_{room}, \right. \\
 &\quad \left. X_{receiver}, Y_{receiver}, Z_{receiver}, X_{equip}, Y_{equip}, Z_{equip} \right) \\
 &= SPL_f(f, p\%, Df, d, m, q, R)
 \end{aligned} \tag{24}$$

a)

where

$$RR_f = \frac{\sum_{i=1}^6 S_i \alpha_{fi}}{1 - \bar{\alpha}_f}; \quad \bar{\alpha}_f = \frac{\sum_{i=1}^6 S_i \alpha_{fi}}{\sum_{i=1}^6 S_i}$$

α_{fi} : the i -th wall's sound absorption coefficient at f -th octave band frequency;

$$S_1 = S_4 = X_{room} * Y_{room}; S_2 = S_5 = Y_{room} * Z_{room}; S_3 =$$

$$S_6 = X_{room} * Z_{room};$$

$$r_1 = \sqrt{(X_{equip} - X_{receiver})^2 + (Y_{equip} - Y_{receiver})^2 + (Z_{equip} - Z_{receiver})^2};$$

$$X_{room}, Y_{room}, Z_{room}, X_{equip}, Y_{equip}, Z_{equip}, X_{receiver}, Y_{receiver}, Z_{receiver}: \text{fixed values.} \tag{24b}$$

Consequently, the overall sound pressure level SPL_T at receiver is

$$SPL_T = \sum_{f=1}^8 10^{SPL_f/10} = SPL_T(p\%, Df, d, m, q, R) \tag{25}$$

By using the formula of Eq.(25), the objective function used in GA optimization with respect to absorber is

$$OBJ = SPL_T(p\%, Df, d, m, q, R) \tag{26}$$

III. MODEL CHECKS

Before performing the GA optimal simulation, the accuracy check of mathematical model on sound absorber is made by experimental data [10]. As depicted in Fig.3, the accuracy comparisons between theoretical and experiment data for the models reveal that they are in good agreement. Therefore, the proposed fundamental mathematical models are acceptable. Thereafter, the models linked with GA optimization method on the constrained sound absorption system are applied as following

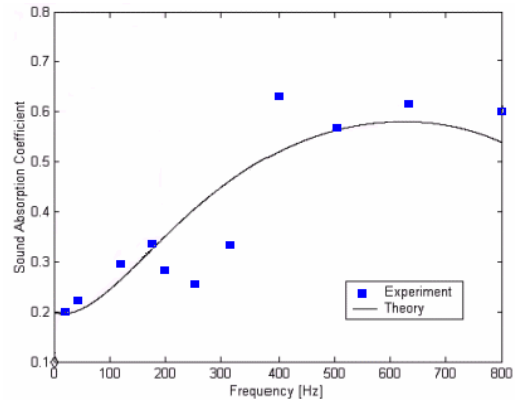


Fig.3 Performance of a single-layer sound absorber[Rockwool;80kg/m³;Do=0.05 (m);q=0.0006(m);p%σ=30(%);d=0.003(m);Df=0.049(m);Galv'd Steel].

IV. GENETIC ALGORITHM

In the following, we give a short description of the genetic algorithm which is applied as the optimizer in the shape optimization of perforated single-layer absorber.

4.1 Populations and chromosome

The initial population is built up by randomization. The parameter set is encoded to form a string which represents the chromosome. By evaluation of the object function, each chromosome is assigned the fitness.

4.2 Parents

By using the probabilistic computation weighted by the relative fitness, pairs of chromosome are selected as parents. The weighted roulette wheel selection is then applied.

4.3 Offspring

One pair of offspring is generated from the selected parent by crossover. Crossover occurs with a probability of pc . Both the random selection of a crossover and combination of the two parent's genetic data are then preceded. The scheme of single-point crossover is chosen in GA's optimization.

4.4 Mutation

Genetically, mutation occurs with a probability of pm of which the new and unexpected point will be brought into the GA optimizer's search domain.

4.5 Elitism

To prevent the best gene from the disappearing and improve the accuracy of

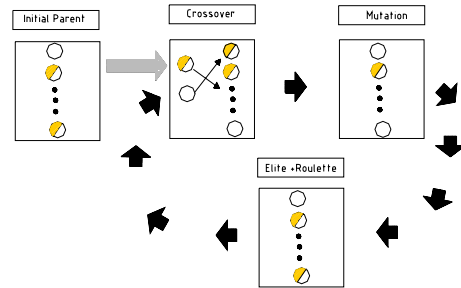


Fig.4 Relations in selection, crossover, mutation and elitism.

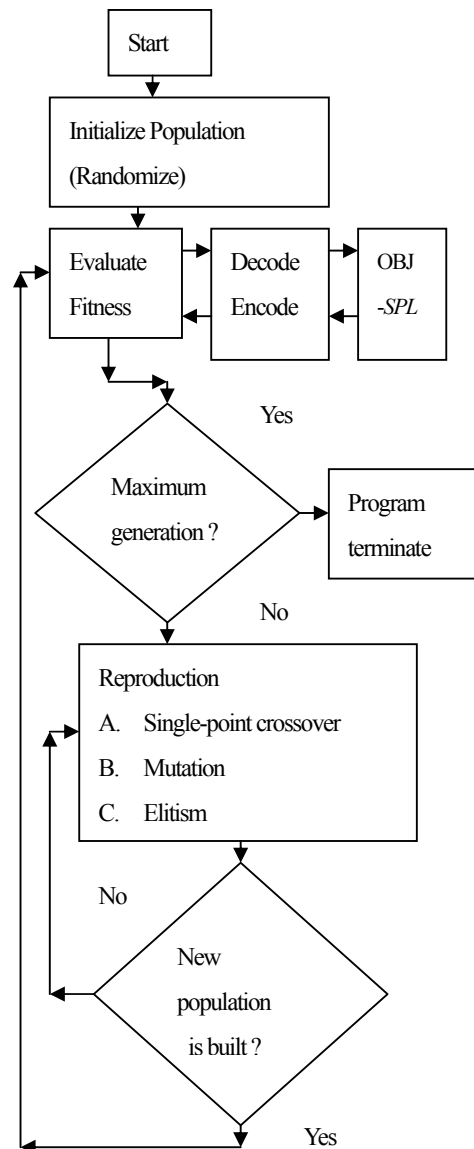


Fig.5 Block diagram of the GA optimization.

optimization during reproduction, the elitism scheme to keep best gene in the parent generations is thus presented and developed.

The relationship in parent selection, crossover, mutation, and elitism is shown in Fig.4.

The GA optimizer developed for sound absorption design on perforated single-layer absorber is depicted in Fig.5.

V. CASE STUDY

In this study, the noise control of a machine room of which the dimensions are 6 meter in length, 6 meter in width and 5 meter in height is introduced and shown in Fig.6.

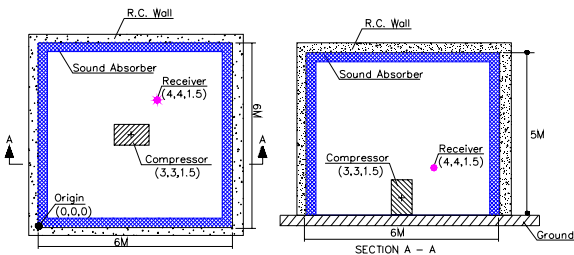


Fig.6 Constrained Sound absorption system by using single-layer absorber.

The noisy equipment's spectrum of SWL (Sound Power Level) is listed as below.

f(Hz)	63	125	250	500	1k	2k	4k	8k
SWL(dB)	90	94	93	104	95	91	88	64

The noisy equipment is located at the

coordination of (3,3,1.5). The thickness (D_o) of single-layer sound absorber, a structure of “rigid-backing plate + L thickness of air + D_f thickness of the acoustic fiber (mineral wool) + q thickness of the perforated front plate”, is fixed to 0.2 (m) for maintenance purpose. To enhance the sound absorption system, the single-layer absorbers are planned to be attached onto four sides of the elevated wall and the ceiling. To efficiently lower the SPL at the receiver of which the coordination is of (3.0,2.0,1.5), an attempt of adjusting the components – the perforated hole of the front plate, perforated ratio, property and thickness of front plate and absorbing material, etc.- is then made under the thickness constraint. In addition, the zone for sound simulation on the plane with 1.5 meter in height is depicted in Fig.7.

For the lightness purpose, the thickness and surface density of absorber's front plate is designed as 0.0006 (m) and 2.0 (kg/m²) respectively. In addition, Rockwool with 80(kg/m³) is chosen as the proposed absorption material filled inside the sound absorber. Furthermore; for the sake of compressibility in Rockwool and availability in front plate's manufacture, all of D_f , $p\%$ and d are specified as 0~0.184 (m), 5~50 (%) and 0.003~0.015 (m) respectively. According to Wang's experiment [11], the flow resistance (R) of above Rockwool is about 22000 (rayle/m). Consequently, the available design parameters of the absorber are then reduced to be D_f , $p\%$ and d .

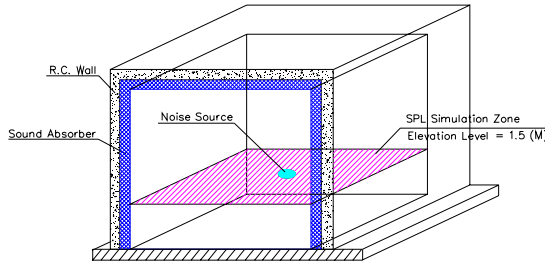


Fig.7 Specified sound simulation zone of h=1.5m within the machine room.

Eqs.(23)~(26) are then reduced as following

$$\alpha_f = 1 - \left| \frac{Z_3 - \rho_o c}{Z_3 + \rho_o c} \right|^2 = \alpha_f(f, p\%, Df, d) \quad (27a)$$

where $L=D_\sigma Df q$; $m=2.0$ (kg/m²); $q=0.0006$ (m); $R=22000$ (rayle/m) (27b)

$$SPL_f = SWL_f + 10 \text{Log} \left[\frac{Q}{4\pi r_1^2} + \frac{4}{RR_f} \right] = SPL_f(f, p\%, Df, d) \quad (28)$$

a)

$X_{\text{room}}=6$ (m); $Y_{\text{room}}=6$ (m); $Z_{\text{room}}=5$ (m);

$$r_1 = \sqrt{\frac{(X_{\text{equip}} - X_{\text{receiver}})^2 + (Y_{\text{equip}} - Y_{\text{receiver}})^2}{(Z_{\text{equip}} - Z_{\text{receiver}})^2}};$$

$(X_{\text{equip}}, Y_{\text{equip}}, Z_{\text{equip}}) = (3, 3, 1.5)$;

$(X_{\text{receiver}}, Y_{\text{receiver}}, Z_{\text{receiver}}) = (3, 2, 1.5)$

(28b)

$$SPL_T = \sum_{f=1}^8 10^{SPL_f/10} = SPL_T(p\%, Df, d) \quad (29)$$

$$OBJ = SPL_T(p\%, Df, d) \quad (30)$$

IV. RESULTS AND DISCUSSION

6.1 Results

The number of population (*popuSize*) is set as 60. The maximum generation (*gen_no*) is set as 500. The bit length is set as 40 (*bit_n*). According to Johnson and Yahya [12], both the typical ratio crossover (*pc*) and mutation ratio (*pm*) used in following GA optimization are chosen as 0.8 and 0.05 respectively. The elite (*elt_no*) is set as optional for the following comparison purpose. To clarify the efficiency in those control parameters including *pc*, *pm* and *elite*, four cases with different values of those control parameters are thus to be discussed. Certainly, other control parameters such as *bit_n*, *popuSize*, *elt_no*, *gen_no* are set to be the same value. Four cases are chosen and defined as follows.

A. Case 1: *pc*=0.8, *pm*=0.05, *elt_no*=1

By using crossover and mutation, the GA optimization is proceeded with elitism. The result shows that the best generation occurred at generation #487. The best values of design parameters-*p%*, *d*, *Df* are found to be 50.0 (%), 0.003 (m) and 0.011133 (m) respectively. The minimized value of sound pressure at receiver is 88.85 dB(A) with respect to these design parameters. In addition, the computation time of optimization process is 1.64 minutes. GA optimization response with respect to

generations is shown in Fig.8.

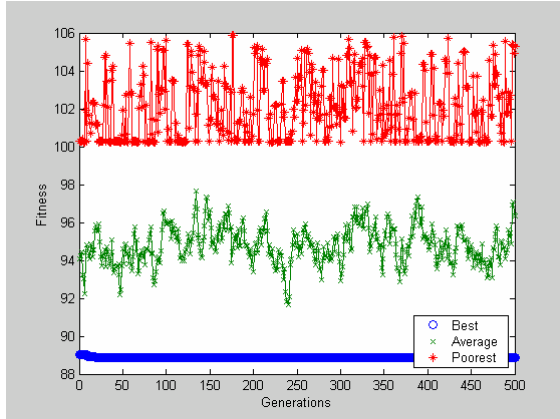


Fig.8 GA optimization response with respect to generations for case 1.

B. Case 2: $pc=0.8, pm=0.05, elt_no=0$

By using crossover and mutation, the GA optimization is proceeded with elitism scheme. The result shows that the best generation occurred at generation #269. The best values of design parameters- $p\%$, d , Df are found to be 49.12 (%), 0.0031 (m) and 0.0089 (m) respectively. The minimized value of sound pressure at receiver is 88.96 dB(A) with respect to these design parameters. In addition, the computation time of optimization process is 1.55 minutes. GA optimization response with respect to generations is shown in Fig.9.

C. Case 3: $pc=0.8, pm=0., elt_no=1$

By using crossover only, the GA optimization is proceeded with elitism scheme. The result shows that the best generation occurred at generation #104. The best values of design parameters- $p\%$, d , Df are found to be 30.45 (%), 0.0039 (m) and 0.01 (m) respectively.

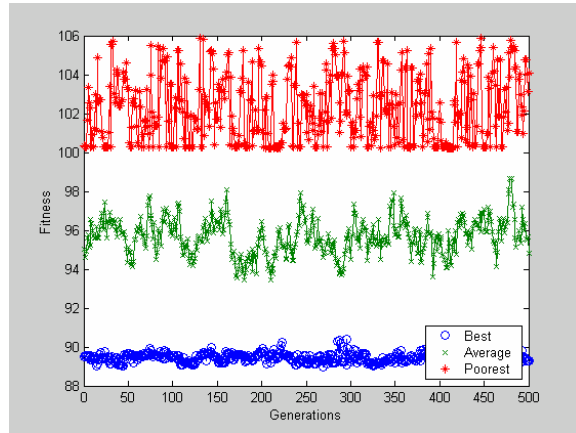


Fig.9 GA optimization response with respect to generations for case 2.

The minimized value of sound pressure at receiver is 89.23 dB(A) with respect to these design parameters. In addition, the computation time of optimization process is 1.58 minutes. GA optimization response with respect to generations is shown in Fig.10.

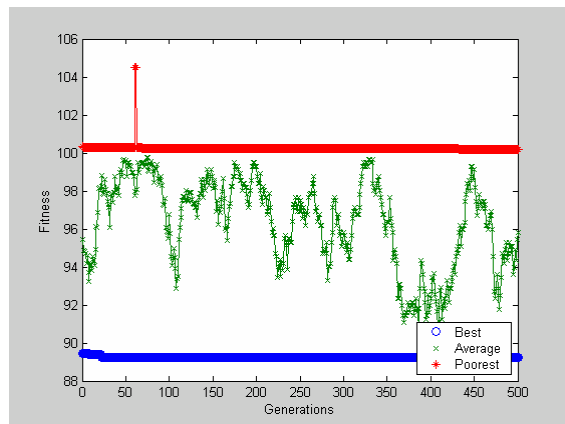


Fig.10 GA optimization response with respect to generations for case 3.

D. Case 4: $pc=0, pm=0.05, elt_no=1$

By using mutation only, the GA optimization is proceeded with elitism scheme.

The result shows that the best generation occurred at generation #133. The best values of design parameters- $p\%$, d , Df are found to be 49.12 (%), 0.0032(m) and 0.0091 (m) respectively. The minimized value of sound pressure at receiver is 88.96 dB(A) with respect to these design parameters. In addition, the computation time of optimization process is 1.55 minutes. GA optimization response with respect to generations is shown in Fig.11.

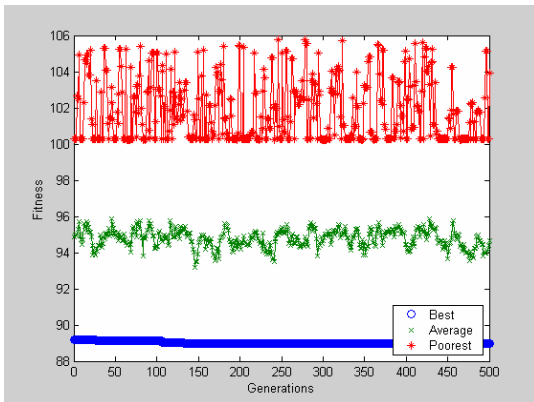


Fig.11 GA optimization response with respect to generations for case 4.

6.2 Discussion

The comparison of optimization in four cases is illustrated in Table 1.

Table 1 indicates that the 1st case of which crossover and mutation/elitism were applied has the better noise reduction of sound pressure level compared with other cases. The sound simulation within the specified zone of $h=1.5$ (m) without adding the sound absorber is plotted in Fig.12.

Table 1 Comparison of results comparison for

the variations of control parameters in GA optimization

	Control parameters			Results				elapse time
	pc	pm	elt_no	$P\%(%)$	$d(m)$	$Df(m)$	SPL	$t(\text{min})$
Case 1	0.8	0.05	1	50.0	0.0030	0.011	88.85	1.64
Case 2	0.8	0.05	0	49.1	0.0031	0.0089	88.96	1.55
Case 3	0.8	0	1	30.4	0.0039	0.010	89.23	1.58
Case 4	0	0.05	1	49.1	0.0032	0.009	88.96	1.55

As indicated in Fig. 12, the slope of the profile at the receiver is flat which means the reverberant noise dominates the sound field. By using the optimized sound absorber, the predicted sound pressure level is shown in Fig.13. As described in Fig. 13, the slope of the profile at the receiving point is much more steeper than that in Fig. 12.

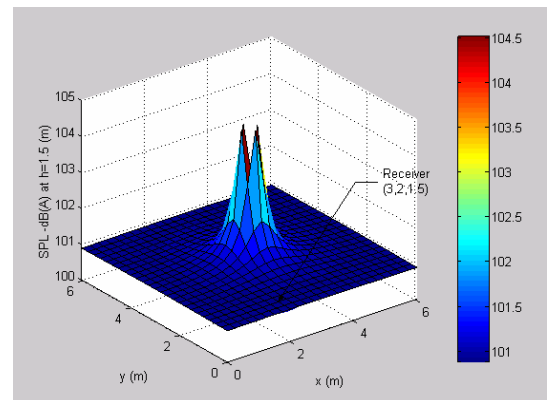


Fig.12 SPL at the specified zone of $h=1.5\text{m}$ before adding sound absorber.

It indicates the direct noise that is inversely proportional to the distance between noise and

receiving points is remarkable. Therefore, it is observed that the reverberant noise inside the room is eliminated efficiently after adding the optimal sound absorber.

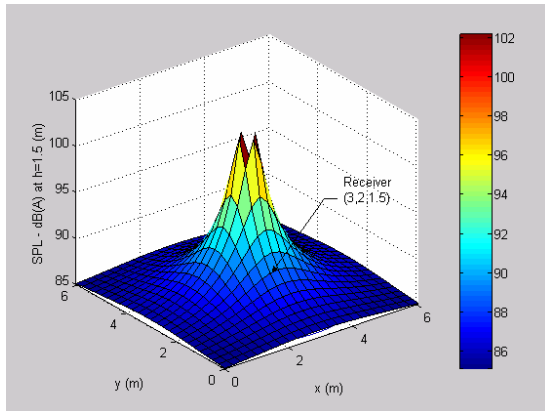


Fig.13 SPL at the specified zone of $h=1.5$ m after adding sound absorber.

VII. CONCLUSIONS

It has been shown that GA can be used in the minimal value of sound pressure level at receiver by adjusting the shape of sound absorber under the space constraints. Because of no starting design, GA becomes easier to be used compared to classical method of which the first derivative and starting point in objective function are required. The case study indicates that all of the GA operators, including crossover, mutation and elitism, are essential and necessary to be considered simultaneously for GA's accuracy purpose. Results summarized reveal that the 1st design case is the best option. In addition, the PC's elapsed times of GA optimization in four cases are short. The penalty cost in computing time is ignorable. This study surely provides a novel scheme with genetic

algorithm in solving the shape optimization of a constrained sound absorption system.

REFERENCES

- [1] Goldberg, D. E., Genetic Algorithm in Search, Optimization and Machine Learning, Addison-Wesley, Massachusetts, 1988.
- [2] Leite, J. P. B., and Topping, B. H. V., "Improve Genetic Operators for Structural Engineering Optimization," *Advances in Engineering Software*, Vol. 29, No.7-9, pp. 529-562, 1998.
- [3] Delany, M. E., and Bazley, E. N., "Acoustical Properties of Fibrous Absorbent Materials," *Applied Acoustics*, Vol. 13, pp.105-116, 1969.
- [4] Ingard, K. U., and Bolt, R. H., "Absorption Characteristics of Acoustic Material with Perforated Facings," *Journal of the Acoustical Society of America*, Vol. 23, pp. 533-540, 1951.
- [5] Bolt, R. H., "On the Design of Perforated Facings for Acoustic Materials," *Journal of the Acoustical Society of America*, Vol. 19, pp. 917-21, 1947.
- [6] Lindfield, G, and Penny, J., Numerical Method Using Matlab, Prentice Hall, 2000.
- [7] Bies, D. A., and Hansen, C. H., Engineering Noise Control, Unwin Hyman, UK, 1988.
- [8] Munjal, M. L., Acoustics of Ducts and Mufflers with Application to Exhaust and Ventilation System Design, John Wiley & Sons, New York, 1987.
- [9] Beranek, L. L., Noise Reduction, McGraw-Hill, New York, 1983.

- [10] Chang, Y. C., Yeh, L. J., and Chiu, M. C., "Optimization on Constrained Single-layer Absorbers by Simulated Annealing," Electronic Journal "Technical Acoustics", 4, pp. 1-13, 2004.
- [11] Wang, C. N., and Tomg, J. H., "Experimental Study of the Absorption Characteristics of Some Porous Fibrous Materials," Applied Acoustics, Vol. 62, pp. 447-459, 2001.
- [12] Johnson, J. M., and Yahya, R. S., "Genetic Algorithm Optimization and Its Application to Antenna Design," Proceedings of the IEEE Antennas and Propagation Society International Symposium, pp. 326-329, 1994.

K_p complex propagation constant of perforated front plate

K_1 real part of complex K_{fiber}

K_2 imaginary part of complex

K_2 imaginary part of complex

m surface density (kg m^{-2})

N hole's number on the perforated front plate per 1m^2

$p\%$ perforated ratio of front plate (%)

p_i acoustic pressure at i (Pa)

q thickness of perforated front plate (m)

R acoustic flow resistance of acoustic fiber (MKS rayls m^{-1})

R_{fiber} real part of complex Z_{fiber}

V_i acoustic mass velocity at i (kg s^{-1})

u_i acoustic particle velocity at i (m s^{-1})

ω angular frequency (rad s^{-1})

Z_i specific normal impedance at

NOMENCLATURE

j $\sqrt{-1}$

c sound speed (m s^{-1})

d diameter of perforated hole on the front plate (m)

D_o thickness of absorber (m)

D_f thickness of acoustic fiber (m)

k wave number

K_{fiber} complex propagation constant of acoustic fiber

	i		pc	crossover ratio
Z_{fiber}		characteristic impedance of acoustic fiber		
Z_p		characteristic impedance of perforated front plate		
X_{fiber}		imaginary part of complex Z_{fiber}		
α		sound absorption coefficient of absorber		
ρ_o		air density (kg m^{-3})		
RR		room constant		
$(X_{room}, Y_{room}, Z_{room})$		Room dimension in x, y and z direction (m)		
$(X_{equip}, Y_{equip}, Z_{equip})$		Coordination of equipment (m)		
$(X_{receiver}, Y_{receiver}, Z_{receiver})$		Coordination of receiver (m)		
bit_n		bit length		
$popuSize$		no. of population		
gen_no		Maximum no. of generation		
elt_no		selection of elite (1 for yes and 0 for no)		
pm		mutation ratio		